

# Analysis and measurement of misalignment effect in inductive-coupling wireless inter-chip connection

**Li Zhang<sup>a)</sup>, Xiaowei Xu, Dawei Li, Jun Zou, and Xuecheng Zou**

*School of Optical and Electronic Information,  
Huazhong University of Science and Technology,  
Wuhan, China*

*a) andyzhang\_ic@163.com*

**Abstract:** Inductive-coupling wireless connection is a promising interconnect technology for 3D stacked chips packaging. Misalignment between inductors of transmitter chip and receiver chip reduces the mutual inductance, leading to a signal transmit failure. A method to evaluate the signal attenuation caused by inductors misalignment is proposed based on the mutual inductance calculation. Misalignment tolerance under constant circuit parameters is given. Test chips are designed and fabricated in 180 nm CMOS process to verify the method. Measurements of the test chip show that the proposed method match well with testing results.

**Keywords:** inductive-coupling, wireless connection, 3D package, misalignment

**Classification:** Integrated circuits

## References

- [1] T. Ezaki, *et al.*: “A 160 Gb/s interface design configuration for multichip LSI,” ISSCC Dig. Tech. Papers (2004) 140 ([DOI: 10.1109/ISSCC.2004.1332633](https://doi.org/10.1109/ISSCC.2004.1332633)).
- [2] J. Burns, *et al.*: “Three-dimensional integrated circuits for low-power, high-bandwidth systems on a chip,” ISSCC Dig. Tech. Papers (2001) 268 ([DOI: 10.1109/ISSCC.2001.912632](https://doi.org/10.1109/ISSCC.2001.912632)).
- [3] K. Kanda, *et al.*: “1.27 Gb/s/pin 3 mW/pin wireless superconnect (WSC) interface scheme,” ISSCC Dig. Tech. Papers (2003) 186 ([DOI: 10.1109/ISSCC.2003.1234260](https://doi.org/10.1109/ISSCC.2003.1234260)).
- [4] R. J. Drost, *et al.*: “Proximity communication,” Proc. of the IEEE CICC (2003) 469 ([DOI: 10.1109/CICC.2003.1249442](https://doi.org/10.1109/CICC.2003.1249442)).
- [5] N. Miura, *et al.*: “Analysis and design of inductive coupling and transceiver circuit for inductive inter-chip wireless superconnect,” IEEE J. Solid-State Circuits **40** (2005) 829 ([DOI: 10.1109/JSSC.2005.845560](https://doi.org/10.1109/JSSC.2005.845560)).
- [6] N. Miura, *et al.*: “Crosstalk countermeasures in inductive inter-chip wireless superconnect,” Proc. of the IEEE CICC (2004) 99 ([DOI: 10.1109/CICC.2004.1358746](https://doi.org/10.1109/CICC.2004.1358746)).
- [7] D. Mizoguchi, *et al.*: “A 1.2 Gb/s/pin wireless superconnect based on inductive inter-chip signaling (IIS),” ISSCC Dig. Tech. Papers (2004) 142 ([DOI: 10.1109/ISSCC.2004.1332634](https://doi.org/10.1109/ISSCC.2004.1332634)).

- [8] X. Xu, *et al.*: “Predictive calculation of coupling coefficient between on-chip small-area multilayer inductors,” ICSICT (2012) 1 ([DOI: 10.1109/ICSICT.2012.6467603](https://doi.org/10.1109/ICSICT.2012.6467603)).
- [9] S. I. Babic and C. Akyel: “Calculating mutual inductance between circular coils with inclined axes in air,” IEEE Trans. Magn. **44** (2008) 1743 ([DOI: 10.1109/TMAG.2008.920251](https://doi.org/10.1109/TMAG.2008.920251)).
- [10] E. R. Joy, *et al.*: “Accurate computation of mutual inductance of two air core square coils with lateral and angular misalignments in a flat planar surface,” IEEE Trans. Magn. **50** (2014) 1 ([DOI: 10.1109/TMAG.2013.2279130](https://doi.org/10.1109/TMAG.2013.2279130)).

## 1 Introduction

3D stacked chips package is one of the most attractive candidates for next generation high-performance large system integration (LSI). In 3D stacked chips package, chips with different processes or functions can be assembled in one package. Chips are stacked and connected by vertical inter-chip connection. Efficient inter-chip connection technology is a key factor to realize high-performance integration.

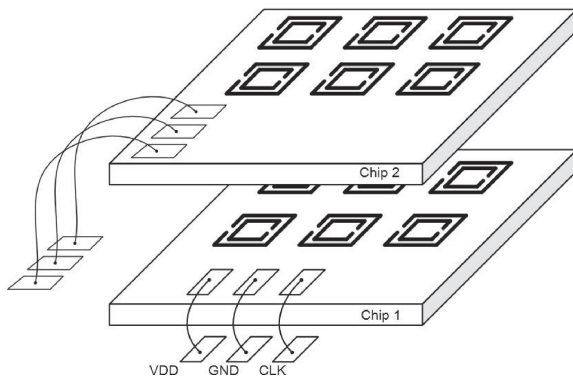


**Fig. 1.** Concept of the 3D stacked chips using inductive-coupling connection.

Several inter-chip connection technologies have been developed, such as micro-bump [1] and through silicon via (TSV) [2]. But they need a series of additional mechanical processes, which may lead to high costs and low yields. Wireless inter-chip connection technologies have been proposed in recent years, including capacitive-coupling connection [3, 4] and inductive-coupling connection [5, 6, 7]. These two kinds of technology are compatible with standard CMOS process and do not require additional mechanical processes. However, capacitive-coupling connection requires chips stacked face-to-face, so it can be only applied to two chips stacked. On the other hand, there is no limitation in inductive-coupling connection implementation, it can be used in communication between more than three stacked chips.

Fig. 1 shows 3D stacked chips using inductive-coupling connection. Chips with different architectures are implemented in one package. High speed AC signals are transmitted by using inductors in every chip, power supply and I/O interface are provided by wire bonding.

Fig. 2(a) shows the transceiver circuit for inductively coupling wireless connection. The transmitter circuit consists of an H-bridge current steering, which determines the direction and magnitude of the current  $I_T$  flowing through the transmitter inductor, according to transmitting data. When the transmitting data, None-return-zero (NRZ) signal, changes from 1 to 0 (or 0 to 1), a fall (or rise) edge is generated in  $I_T$ . In the receiver circuit, positive or negative pulse voltage  $V_R$  is induced in the receiver inductor, corresponding to the change of  $I_T$ . Then  $V_R$  is recovered to a NRZ signal by an amplifier and a latching circuit. Waveform of the transceiver is shown as Fig. 2(b).

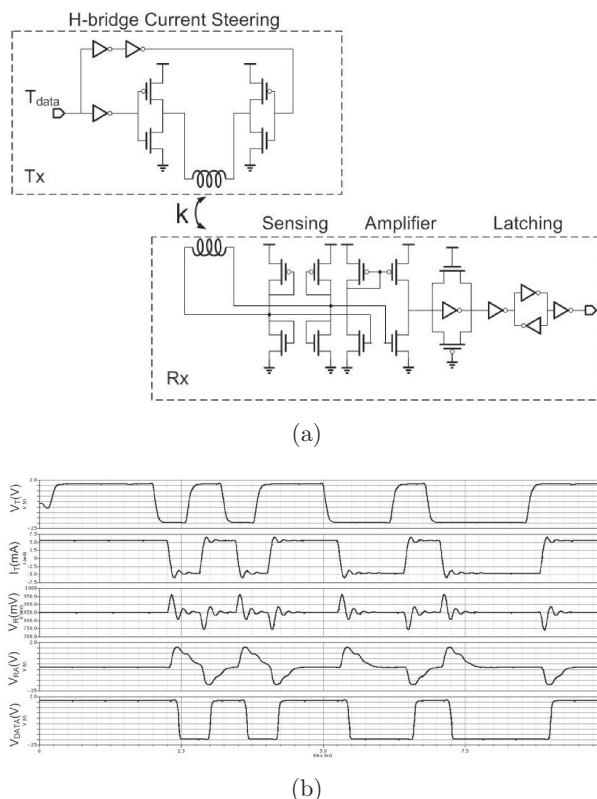


**Fig. 2.** (a) Transceiver circuit of inductive-coupling connection  
(b) Waveform of transceiver circuit

Fig. 3 shows the concept of  $V_R$  attenuation due to the misalignment of stacked chips. Because of the misalignment, less magnetic flux generated by the transmitter inductor can penetrate the receiver inductor. As a result, the induced voltage in the receiver inductor is attenuated. To ensure the data is being received correctly, the misalignment should be limited to a range. In this research, a model for estimating the misalignment tolerance is proposed.

This paper is organized as follows. In Section 2, the misalignment effect evaluation method in inductive-coupling connection is introduced. In Section 3, the design and measurements of test chips are described. In Section 4, analysis of the comparison between measurement results and the proposed method is presented. Conclusions of this paper are provided in section 5.

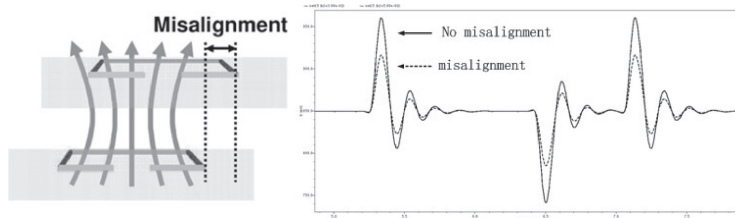


Fig. 3. Receiver voltage attenuation caused by misalignment

## 2 Misalignment effect evaluation

The induced voltage in the receiver is given by

$$V_R = M \frac{dI_T}{dt} \quad (1)$$

Where  $M$  is the mutual inductance between transmitter inductor and receiver inductor.  $I_T$  is the current flows in transmitter inductor, and  $t$  is the propagation delay. Obviously, when the parameters of circuit are specified,  $V_R$  is proportional to  $M$ .

The mutual inductance of rectangle coils with misalignment is calculated by the Biot-Savart law. The spiral inductor can be simplified to a closed rectangle coil, because its outer diameter and inner diameter are usually approximate [8]. As Fig. 4, The Z-axis direction component of the magnetic flux density produced by segments a and c is given by Eq. (2)

$$\begin{aligned} B_{a,c} = & \frac{\mu_0}{4\pi} \frac{x}{x^2 + z^2} \left( \frac{y}{\sqrt{x^2 + y^2 + z^2}} + \frac{D - y}{\sqrt{x^2 + (D - y)^2 + z^2}} \right) \\ & + \frac{\mu_0}{4\pi} \frac{D - x}{(D - x)^2 + z^2} \left( \frac{D - y}{\sqrt{(D - x)^2 + (D - y)^2 + z^2}} \right. \\ & \left. + \frac{y}{\sqrt{(D - x)^2 + y^2 + z^2}} \right) \end{aligned} \quad (2)$$

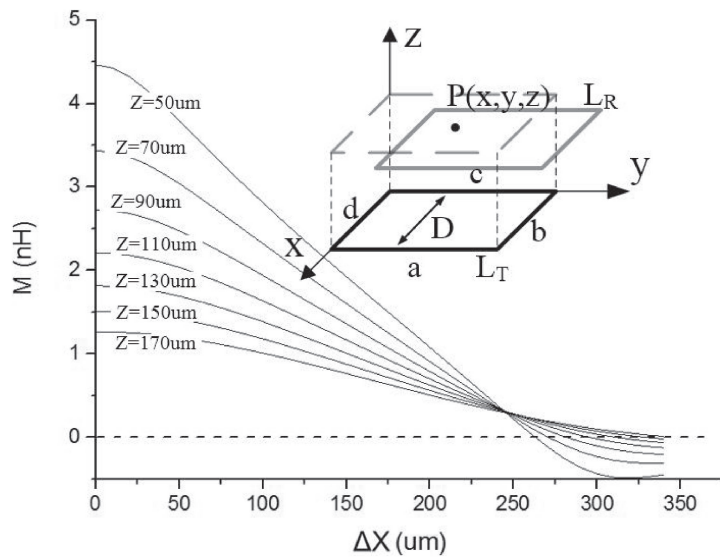


Fig. 4. Mutual inductance calculated result dependence on  $\Delta X$  with different communicate distances.

Where  $\mu_0$  is the permeability of free space, and the current in the coil is unit.  $D$  is the diameter of inductor.  $(x, y, z)$  is the coordinate of the point  $P$  in the area. Subsequently, the mutual inductance in the receiver inductor  $L_R$  can be calculated by Eq. (3)

$$M_{a,c} = \phi_{a,c} = \iint_{L_R} B_{a,c} = \int_{\Delta X}^{\Delta X+D} \int_0^D B_{a,c} dy dx \\ = \frac{\mu_0}{2\pi} \begin{cases} \sqrt{(\Delta X + D)^2 + D^2 + Z^2} + \sqrt{(\Delta X - D)^2 + D^2 + Z^2} \\ -2\sqrt{\Delta X^2 + D^2 + Z^2} - \sqrt{(\Delta X + D)^2 + Z^2} \\ -\sqrt{(\Delta X - D)^2 + Z^2} + 2\sqrt{\Delta X^2 + Z^2} \\ -D \cdot \operatorname{arctanh} \frac{D}{\sqrt{(\Delta X + D)^2 + Z^2 + D^2}} \\ -D \cdot \operatorname{arctanh} \frac{D}{\sqrt{(\Delta X - D)^2 + Z^2 + D^2}} \\ +D \cdot \operatorname{arctanh} \frac{D}{\sqrt{\Delta X^2 + Z^2 + D^2}} \end{cases} \quad (3)$$

Where  $\Delta X$  is the misalignment on X-axis direction,  $Z$  is the distance between  $L_T$  inductor and  $L_R$  inductor.  $\operatorname{arctanh}$  is the arc-hyperbolic function,  $\operatorname{arctanh} x = \frac{1}{2} \ln \frac{1+x}{1-x}$ .

So as the segments b and d

$$B_{b,d} = \frac{\mu_0}{4\pi} \frac{y}{y^2 + z^2} \left( \frac{x}{\sqrt{x^2 + y^2 + z^2}} + \frac{D - x}{\sqrt{(D - x)^2 + y^2 + z^2}} \right) \\ + \frac{\mu_0}{4\pi} \frac{D - y}{(D - y)^2 + z^2} \left( \frac{D - x}{\sqrt{(D - x)^2 + (D - y)^2 + z^2}} \right. \\ \left. + \frac{x}{\sqrt{x^2 + (D - y)^2 + z^2}} \right) \quad (4)$$

$$\begin{aligned}
 M_{b,d} = \phi_{b,d} &= \iint_{L_R} B_{b,d} = \int_{\Delta X}^{\Delta X+D} \int_0^D B_{b,d} dy dx \\
 &= \frac{\mu_0}{2\pi} \left( \begin{array}{l}
 \sqrt{(\Delta X + D)^2 + D^2 + Z^2} + \sqrt{(\Delta X - D)^2 + D^2 + Z^2} \\
 -2\sqrt{\Delta X^2 + D^2 + Z^2} - \sqrt{(\Delta X + D)^2 + Z^2} \\
 -\sqrt{(\Delta X - D)^2 + Z^2} + 2\sqrt{\Delta X^2 + Z^2} \\
 -(\Delta X + D) \cdot \operatorname{arctanh} \frac{\Delta X + D}{\sqrt{(\Delta X + D)^2 + Z^2 + D^2}} \\
 -|\Delta X - D| \cdot \operatorname{arctanh} \frac{|\Delta X - D|}{\sqrt{(\Delta X - D)^2 + Z^2 + D^2}} \\
 +2\Delta X \cdot \operatorname{arctanh} \frac{\Delta X}{\sqrt{\Delta X^2 + Z^2 + D^2}} \\
 +(\Delta X + D) \cdot \operatorname{arctanh} \frac{\Delta X + D}{\sqrt{(\Delta X + D)^2 + Z^2}} \\
 +|\Delta X - D| \cdot \operatorname{arctanh} \frac{|\Delta X - D|}{\sqrt{(\Delta X - D)^2 + Z^2}} \\
 +2\Delta X \cdot \operatorname{arctanh} \frac{\Delta X}{\sqrt{\Delta X^2 + Z^2}}
 \end{array} \right) \quad (5)
 \end{aligned}$$

The total mutual inductance is

$$M = n(M_{a,c} + M_{b,d}) \quad (6)$$

$n$  is the total turns number of two inductors. The  $\Delta X$  in Eq. (3) and Eq. (5) can be replaced by a misalignment on any direction in the x-y plane, it makes an error below 5%.

Fig. 4 shows the calculated mutual inductance dependence on  $\Delta X$  with different distance. Diameter of inductors is 300  $\mu\text{m}$ ,  $L_R$  and  $L_T$  are both 4 turns, corresponding to the size of inductors on test chips in next section. The mutual inductance decreases along with the growth of misalignment. When it is under 0, the direction of magnetic flux penetrating the receiver inductor changes. It means that the polarity of the received signal is inverted.

The reduction of  $V_R$  caused by misalignment can be compensated by increasing  $I_T$ , by another word, consuming more transmitter energy. Normalized required transmitter energy is given by

$$E(\Delta X, Z) = \frac{M(0, Z_0)}{M(\Delta X, Z)} \quad (7)$$

$Z_0$  is the initial  $Z$  of calculating. Normalized required transmitter energy depends on  $\Delta X/D$  and  $Z/D$  is shown in Fig. 5.

### Crosstalk in channels array

To obtain a high bandwidth, channels of the inductive-coupling connection are usually arranged in array. The compact arrangement causes crosstalk between inductors. The effect of crosstalk is shown in Fig. 6(a). The  $R_X$  inductor receives the signal from the  $T_X$  inductor while also receiving interference from inductors

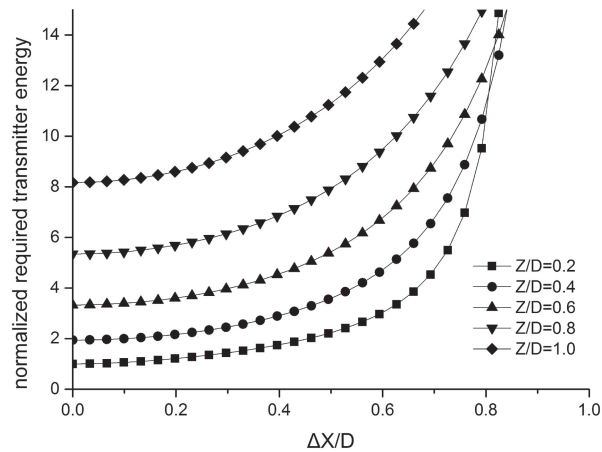


Fig. 5. Normalized required transmitter energy dependence on  $\Delta X$  with different communicate distances.

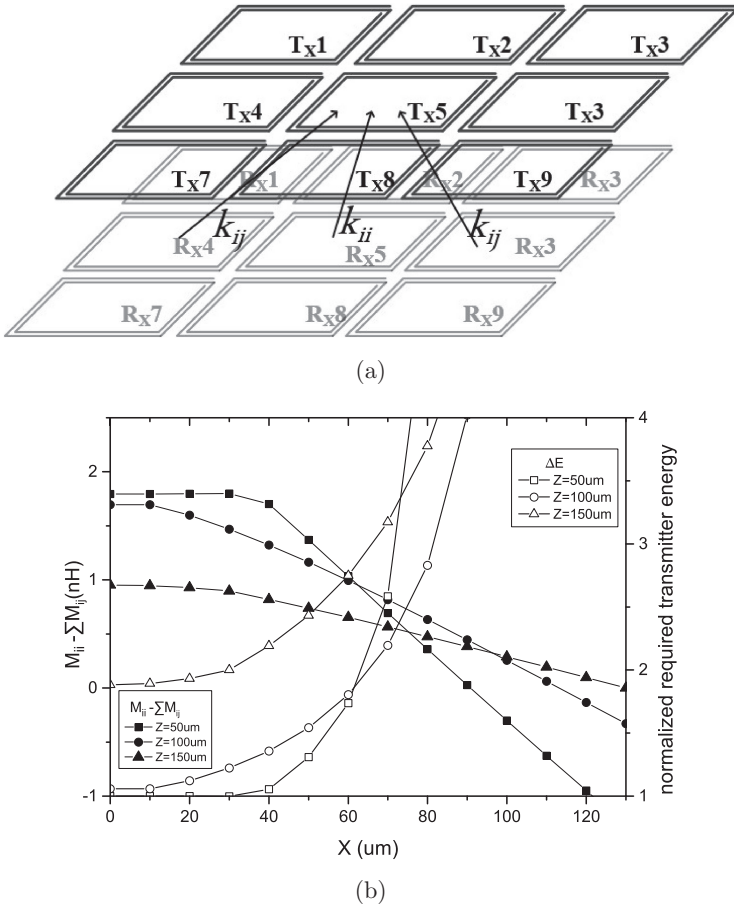


Fig. 6. (a) Concept of crosstalk (b)  $M_{ii} - \sum M_{ij}$  and normalized required transmitter energy depends on  $\Delta X$  in a  $3 \times 3$  array

around the  $T_X$  inductor. When inductors are misaligned, the received signal decreases, and the crosstalk increases. This change is demonstrated by Eq. (8)

$$V_R = \left( M_{ij} \downarrow + \sum_{j=0}^n a_{ij} \cdot |M_{ij}| \uparrow \right) \frac{dI_T}{dt} \quad (8)$$

Where  $M_{ij}$  is the mutual inductance between the  $i$ th receiver ( $R_{Xi}$ ) and  $j$ th transmitter ( $T_{Xj}$ ) inductor.  $a_{ij}$  is the direction of the interference, can be the value of  $-1$ ,  $+1$  or  $0$  based on data transitions in each transmitted data. To discuss the worst scenario, assuming that the direction of the interference signal is contrary to the original signal, which means all  $a_{ij}$  are equal to  $-1$ . The reduction of  $V_R$  caused by misalignment in array arrangement is also can be compensated by increasing the transmitter energy, the normalized required energy is calculated by Eq. (9)

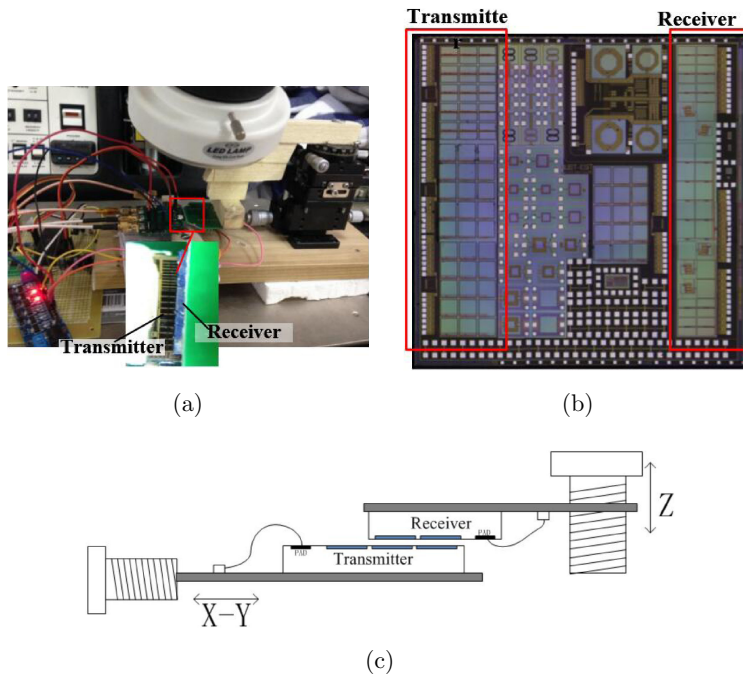
$$E_{array}(\Delta X, Z) = \frac{M_{ii}(0, Z_0) - \sum M_{ij}(0, Z_0)}{M_{ii}(\Delta X, Z) - \sum M_{ij}(\Delta X, Z)} \quad (9)$$

Fig. 6(b) shows the calculated  $M_{ii} - \sum M_{ij}$  and normalized required transmitter energy depends on  $\Delta X$  with different communicate distance in a  $3 \times 3$  array. The mutual inductance is changing rapidly and complicatedly under the affect of misalignment.

### 3 Test chip design and measurement setup

Test chips were designed and fabricated in  $180\text{ }\mu\text{m}$  CMOS technology. Fig. 7(a) shows the micro-photograph stacked chips. The inductors on chip have 4 turns, and their size is  $300\text{ }\mu\text{m}$ . Both transmitter inductors and receiver inductors are arranged in arrays compactly. They can work alone or together controlled by switches, to test the performance without or with crosstalk, respectively.

Fig. 7(b) and Fig. 7(c) shows the measurement setup. The transmitter chip and receiver chip are stacked face-to face. The transmitter chip is face-up and connected to the working platform. The receiver chip is face-down and mounted on the operation handle, which can be moved in both vertical and horizontal directions. These inductors are fabricated with the first and second top metal layer on chip,



**Fig. 7.** (a) Test implementation (b) Test chip microphotograph (c) Concept of implementation movement

the distance between two chips can be considered equal to the distance between transmitter inductors and receiver inductors. Transmitter current  $I_T$  can be adjusted from 1 mA to 8 mA by controlling the gates of H-bridge current steering.

#### 4 Test result

Fig. 8 shows the misalignment tolerance with different distances and variable transmitter current, without crosstalk. The bit rate is 100 Mbit/s, and the bit error rate is set to less than  $10^{-9}$ . The transmitter current 2 mA, 4 mA, 6 mA, 8 mA are corresponding to transmit energy 1.8 mW/channel, 3.6 mW/channel, 5.4 mW/channel, 7.2 mW/channel, respectively. The dash line curve in Fig. 8 is the calculated contour of the mutual inductance. It can be seen that each misalignment tolerance boundary of variable current is along with a mutual inductance line, which makes the product of  $I_T$  and  $M$  is a constant (nearly equal to 6.4). Put these points of test result in the normalized figure, shown as Fig. 9, they also match the calculated result well. This results indicates that the misalignment tolerance of inductive coupling connection is large enough, because the misalignment under  $0.2 \cdot D$  can be compensated by energy increasing below 20%.

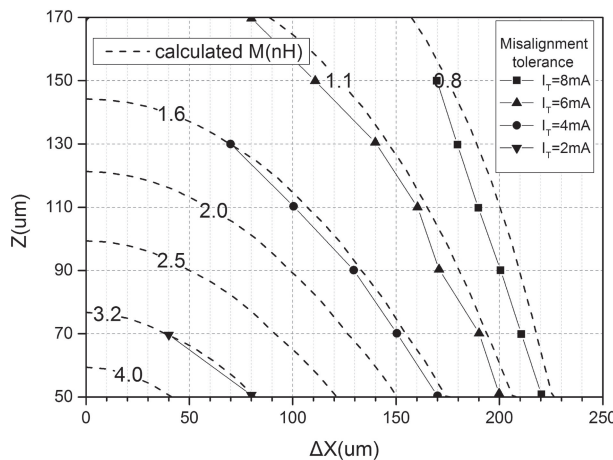


**Fig. 8.** Measured misalignment tolerance and calculated mutual inductance

Fig. 10 shows the misalignment tolerance of an inductive coupling connection channel that works in a  $3 \times 3$  array. The error of test result is larger than that in Fig. 8, because this condition is much more complicated. The lateral and angel misalignment mentioned in [9, 10] may be affect the result a lot.

With the crosstalk, the misalignment tolerance is much smaller than that when channel worked alone. Much more energy is required to compensate the attenuation of  $V_R$ . Extending the pitch of inductors array is a effective way to weaken the effect of misalignment. Calculated by can eq. (10), extending the pitch to  $2 \cdot D$  can weaken the the effect of crosstalk down to 10%.

$$\text{crosstalk-to-signal} = \frac{\sum M_{ij}(\text{pitch}, D, Z)}{M_{ii}(D, Z)} \quad (10)$$

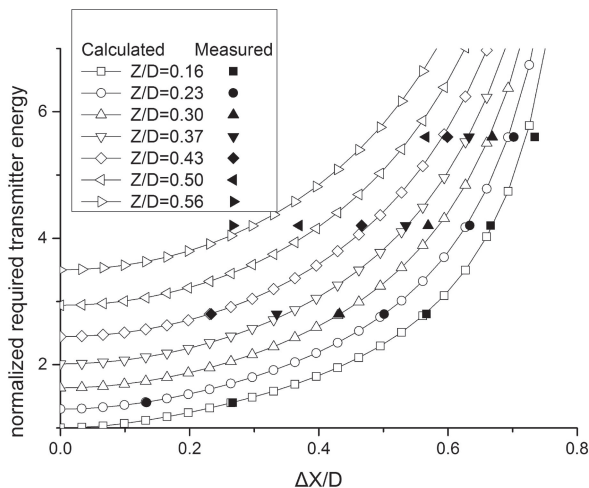


Fig. 9. Normalized result

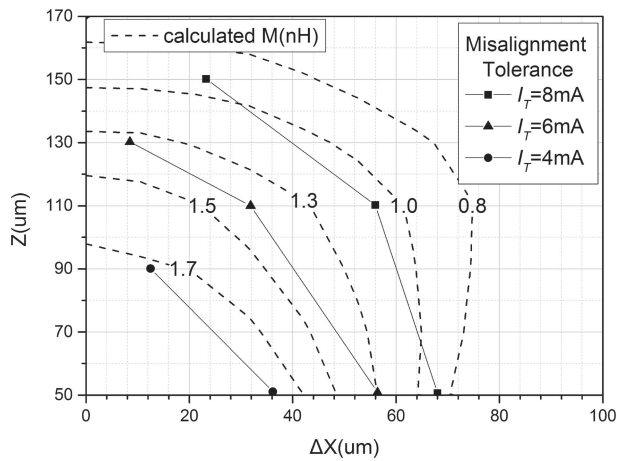


Fig. 10. Measured misalignment tolerance and calculated mutual inductance with crosstalk

## 5 Conclusions

One method based on mutual inductance calculation to evaluate the misalignment tolerance in inductive-coupling connection is introduced. The test chip is designed for verifying the method. When the calculated result was compared with the measured result, the method was found to be accurate. The result shows that the misalignment tolerance in inductive-coupling connection can be high enough to keep performance in common case, but requirement of alignment in inductor array is much stricter.

## Acknowledgments

This work is supported by National Natural Science Foundation of China (Grant No. 61376031).